Nano-Optical Imaging Spectroscopy: Recent Advances in Near-field Scanning Optical Microscopy

Toshiharu Saiki* and Yoshihito Narita**

Abstract

Current progress in the instrumentation and measurements of near-field scanning optical microscopy (NSOM) is described. The most critical element in NSOM is an aperture probe, which is a tapered and metal-coated optical fiber. The design and fabrication of the probe are examined with regard to aperture quality and the efficiency of light propagation. The recent dramatic improvements in spatial resolution and optical throughput are illustrated by selected applications, including ultrafast coherent spectroscopy, Raman spectroscopy, polarization microscopy, and the emission imaging of semiconductor nanostructures and single molecules. These examples demonstrate that NSOM has developed into a powerful tool for study on a new frontier of science.

1. Introduction

As an eye on the nanoscale world, optical microscopy with high spatial resolving power is indispensable in a wide range of science and technology. In material science, for example, local optical properties that depend on the microscopic complexity and heterogeneity of materials need to be characterized on the nanometer scale. And the nanoenvironment of biosystems can be identified by monitoring the fluorescent behavior of an individual molecule. While the conventional optical microscope provides excellent spectral and temporal selectivity, its spatial resolution is limited by diffraction to roughly half the wavelength of the illuminating light. Today, however, we need tools that can locate, distinguish, and characterize features whose size and separation are small compared to the wavelength of light. Electron microscopy, scanning tunneling microscopy (STM), and atomic force microscopy (AFM) provide atomic-scale resolution and can be used to manipulate atoms and nanostructures but are not particularly suitable for the observation of spectral and dynamic properties.

Resolution beyond the diffraction limit is usually obtained by using near-field scanning optical microscopy (NSOM), in which a small aperture (a scatterer) providing illumination is scanned close to the object under observation.[1,2] The progress in probe fabrication techniques has made routine procedures of optical imaging and spectroscopy with a resolution of 100 nm. It is also possible, with a high-quality probe, to reach a resolution of approximately 10 nm. The highly resolved topographic mapping obtained simultaneously with the optical images is as important as those images and is especially helpful in biological applications, where samples often exhibit complex morphology. Furthermore, the combination of NSOM and ultrafast excitation by a pulsed laser has advantages over STM and AFM because the temporal resolution provided by this combination is in the femtosecond regime. NSOM has thus become a valuable tool applicable for a wide range of studies in physics, chemistry, and biology.

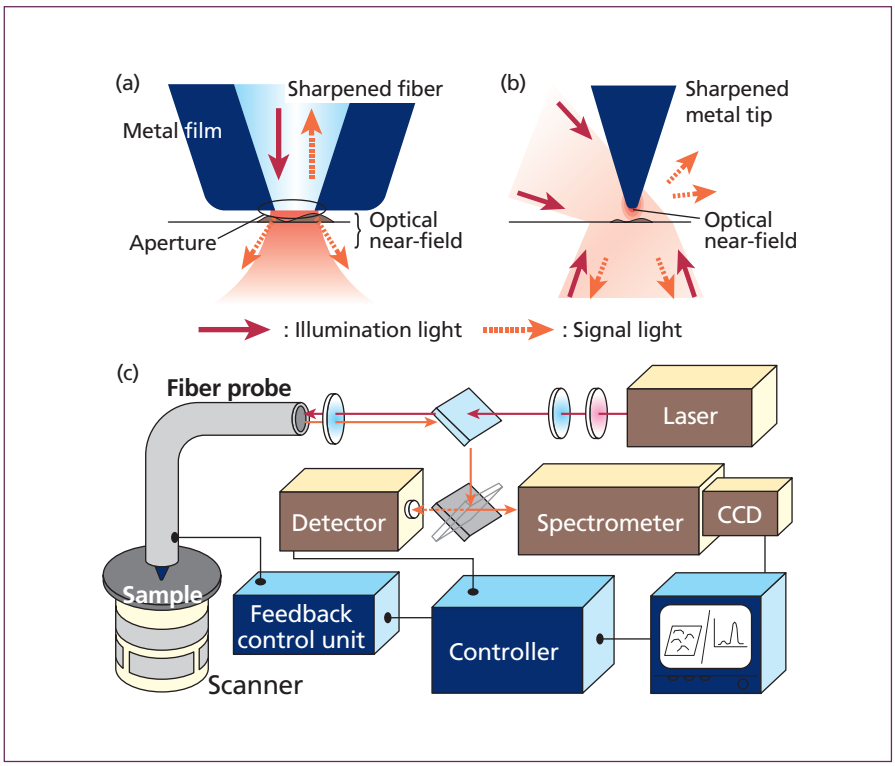

Fig. 1 Schematic illustration of (a) aperture NSOM and (b) apertureless (scattering) NSOM. (c) Schematic of standard NSOM setup with a local illumination and local collection configuration.

2. General description of NSOM

When a small object is illuminated, its fine structures with high spatial frequency generate a localized field that decays exponentially normal to the object. This evanescent field on the tiny substructure can be used as a local source of light illuminating and scanning a sample surface so close that the light interacts with the sample without diffracting. There are two methods by which a localized optical field suitable for NSOM can be generated. As illustrated in Fig. 1(a), one method uses a small

* Department of Applied Physics, University of Tokyo, Tokyo 113-8656, Japan
Special Research Laboratory for Optical Science, Kanagawa Academy of Science and Technology, Kawasaki, Kanagawa 213-0012, Japan
** Spectroscopic Products Division, JASCO Corporation, Hachioji, Tokyo 192-8537, Japan

aperture at the apex of a tapered optical fiber coated with metal. Light sent down the fiber probe and through the aperture illuminates a small area on the sample surface. The fundamental spatial resolution of aperture NSOM is determined by the diameter of the aperture, which ranges from 10 to 100 nm.

In the other method, called apertureless (or scattering) NSOM and illustrated in Fig. 1(b), a strongly confined optical field is created by external illumination at the apex of sharpened metal or dielectric tip. Spatial resolution approaching the atomic scale is expected, and laboratory experiments have yielded resolutions ranging from 1 to 20 nm. A rather large (diffraction limited) laser spot focused on a tip apex frequently causes an intense background that reduces the signal-to-noise ratio. This contrasts with what is done in aperture NSOM, where the aperture serves as a localized light source without any background. The general applicability of the apertureless method to a wide range of samples is currently being investigated.

The simplest setup for aperture NSOM, a configuration with local illumination and local collection of light through an aperture, is illustrated in Fig. 1(c). The probe quality and the regulation system for tip-sample feedback are critical to NSOM performance, and most NSOMs use a method similar to that used in an AFM, called shear force feedback, the regulation range of which is 0-20 nm. The light emitted by the aperture interacts with the sample locally. It can be absorbed, scattered, or phase-shifted, or it can excite fluorescence. Which of these occur(s) depends on the sample and produce(s) contrast in the optical images. In any case, light emerging from the interaction volume must be collected as efficiently as possible. When the sample is prepared on a transparent substrate, signal light is frequently collected with an objective lens arranged in a transmission configuration.

3. Fabrication of aperture probe

Great efforts have been devoted to the fabrication of the aperture probe, which is at the heart of NSOM. Since the quality of the probe determines the spatial resolution and sensitivity of the measurements, tip fabrication remains of major interest in near-field optics. The fabrication of fiber-based optical probes can be divided into the three main steps illustrated in Fig 2: (a) the creation of a taper structure with a sharp apex, (b) coating with a metal (Al, Au, Ag) to obtain an entirely opaque film on the probe, and (c) the formation of a small aperture at the apex.

There are two methods used to make tapered optical fibers with a sharp tip and reasonable cone angle. One is the heating-and-pulling method, where the fiber is locally heated using a CO_2 laser and is subsequently pulled apart. The other method, based on chemical etching in a hydrofluoric acid (HF) solution, is more reproducible production and can be used to make many probes at the same time.[3,4] A specific advantage of the chemical-etching method is that the taper angle, which determines the efficiency of light transmission and will be discussed in the following section, can be adjusted by changing the composition of a buffered HF solution. Another important advantage is the excellent stability of the polarization state of the probe. When the heating-and-pulling method is used, in contrast, temporal fluctuation of polarization occurs due to relaxation of strain induced by the production process.

The technique most often used to form a small aperture is based on the geometrical shadowing method used in the evaporation

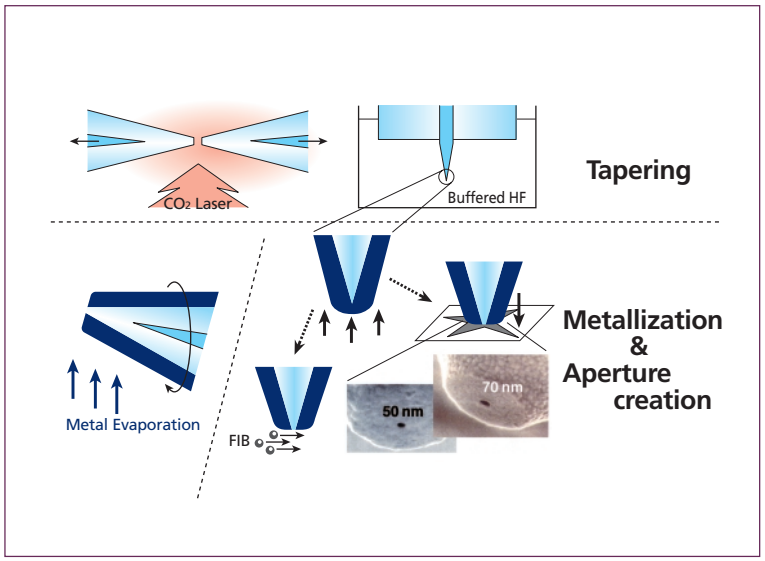

Fig. 2 Fabrication of an aperture NSOM probe: creation of taper structure, metallization of exterior surface, and formation of aperture at the apex. The inset shows scanning electron micrographs of 50-nm and 70-nm apertures made by the impact method.

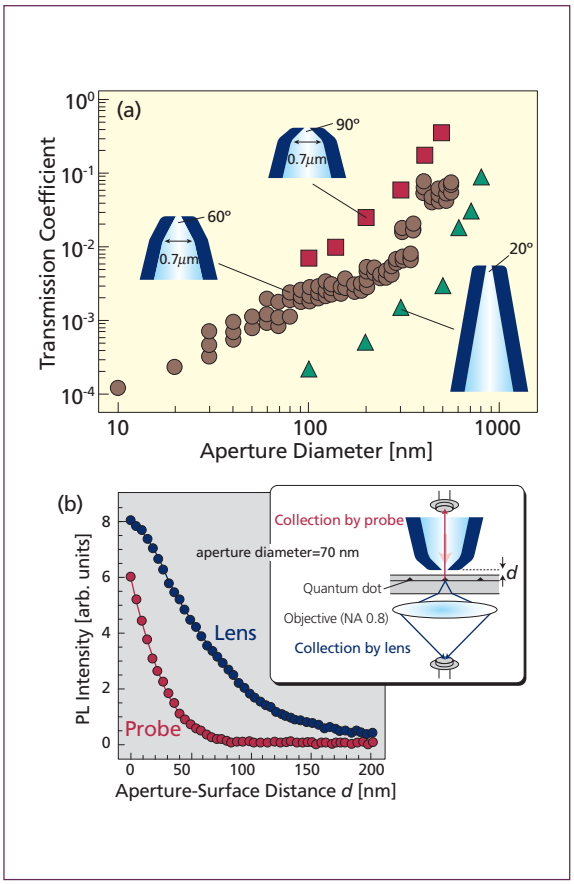

Fig. 3 (a) Plots of transmission coefficient of aperture probe as a function of aperture diameter for single-tapered and double-tapered probes with cone angles of 60° and 90°. A He-Ne laser with a wavelength of 632.8 nm was used for this measurement. (b) Comparison of collection efficiency of an objective and a probe with a 70-nm aperture. Photoluminescence intensities collected from a single quantum dot are plotted as a function of distance between the aperture and the surface.

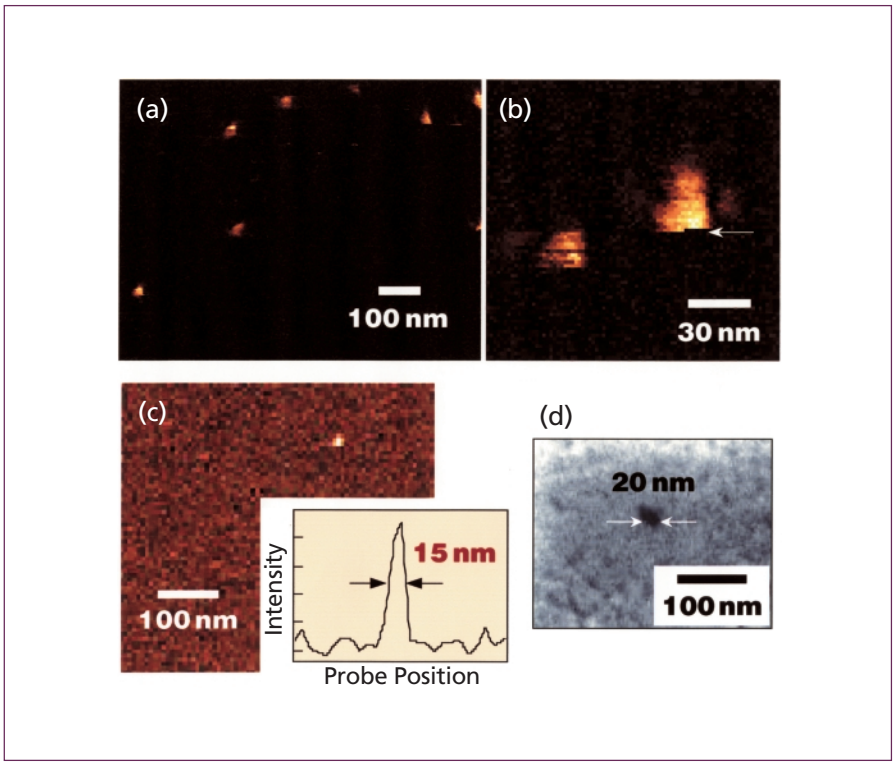

Fig. 4 (a) Typical near-field fluorescence image of single dye molecules. (b) Magnified view of one of the bright spots in part (a). Irreversible photobleaching occurred at the moment indicated by the arrow. (c) One of the highest-resolution images obtained by using a 20-nm aperture whose diameter was determined as shown by the scanning electron micrograph in part (d).

of metal. Since the metal is evaporated at an angle from behind, the coating rate at the apex is much smaller than that on the sides. The evaporated metal film generally has a grainy texture, resulting in an irregularly shaped aperture with asymmetric polarization behavior. The grains also increase the distance between the aperture and the sample, not only degrading resolution but also reducing the intensity of the local excitation. A method for making a high-definition aperture probe by milling and polishing using a focused ion beam has been developed,[5] as has a simple method based on the mechanical impact of the tip on a suitable surface.[6] In both methods, the resulting probe has a flat end and a well-defined circular aperture. Furthermore, the impact method assures that the aperture plane is strictly parallel to the sample surface, which is important in minimizing the distance between the aperture and the sample surface.

4. Transmission efficiency of the aperture probe

To achieve the ultimate performance in aperture NSOM, the throughput of light as well as the quality of the aperture should be optimized. In addition to contributing to the high sensitivity of NSOM measurements, optical probes with high transmission efficiency will open up attractive new areas of research, such as nonlinear processes and optical manufacturing on the nanometer scale. It is therefore of great importance to understand the limitations and possibilities of aperture probes with respect to light transmission.

The tapered region of the aperture probe is considered to be a metal-clad optical waveguide. The mode structure in a metallic waveguide is completely different from that in an unperturbed fiber and is characterized by the cutoff diameter and absorption coefficient of the cladding metal. Theoretical and systematic experimental studies have confirmed that the transmission efficiency of the propagating mode decreases in the region where the core diameter is smaller than half the wavelength of the light in the core. The power that is actually delivered to the aperture depends on the distance between the aperture plane and the plane in which the probe diameter is equal to the cutoff diameter, which distance is determined by the cone angle of the taper. We therefore proposed a double-tapered structure with a large cone angle (insets in Fig. 3 (a)).[7] This structure is easily realized using a multi-step HF etching technique. In Fig. 3(a) the transmission coefficient (the ratio of the light power emitted by the aperture to the power coupled into the fiber) is plotted against aperture diameter for conventional single-tapered probes and for double-tapered probes with different cone angles. It is clear that the transmission efficiency of the double-tapered structure with a large cone angle is two orders of magnitude greater than that of the single-tapered probe with a small cone angle. More sophisticated structures, such as a triple-tapered probe, have also been proposed for specific applications.[8,9]

Superior collection of the locally emitted signal is important for the observation of opaque materials like semiconductors. The collection efficiency of the 70-nm aperture probe is compared with that of an objective in Fig. 3(b), where the photoluminescence intensity collected from a single quantum dot is plotted as a function of distance between the aperture and the surface. Within 15 nm of the surface, the amount of light collected by the aperture probe increases rapidly and reaches a value as great as the amount collected by an objective with a numerical aperture of 0.8. This suggests that fabrication of the flat-ended probe makes a considerable contribution to the efficient interaction of the aperture and evanescent field in the vicinity of the sample.

The overall throughput (or collection efficiency) of light is determined by various factors such as the wavelength of propagating light and the corresponding dielectric constant of the cladding metal, as well as by the structure of unperturbed fiber. Numerical analysis and computational simulation of light propagation is a useful and efficient way to obtain the information needed to make an optimized structure.[10,11]

5. Fluorescence imaging spectroscopy

NSOM fluorescence measurements are the simplest and most informative method because they provide high-contrast imaging of nanostructures, revealing the chemical composition and molecular structure as well as the defects and dopants in semiconductors. High-resolution optical imaging of biological samples with fluorescence labels is also a promising field of application. NSOM has the potential to image the distribution of such labels down to the

level of single fluorophores. Furthermore, the presence of the probe (metal aperture) alters the fluorescence lifetime and emission pattern, making it possible to control radiation in the immediate vicinity of the probe (i.e., locally within the nanoenvironment).

Although NSOM offers attractive possibilities with regard to the detection of single molecules, the current spatial resolution of 100 nm is not sufficient for application to actual biological samples. Imaging with a very small aperture (<30 nm) has often been impossible because the transmission efficiency decreases drastically with aperture diameter. Moreover, even a small grain on the aperture plane is problematic because the consequent increase of the aperture-sample distance reduces the spatial resolution. As mentioned in the previous section, however, tailored probes with a high-quality aperture have solved this problem.

We have made fluorescence images of single dye molecules by using an aperture significantly smaller than usual.[12] Cy 5.5 molecules were dispersed on a quartz substrate and illuminated by He-Ne laser light through an aperture made of gold. The fluorescence from a single molecule was collected by the same aperture or by an objective in transmission configuration. Figure 4(a) shows a typical fluorescence image of individual molecules, and Fig. 4(b) is a magnified view of one of the bright spots in Fig. 4(a). The diameter of each spot was estimated to be 30 nm, which corresponds to the aperture diameter produced by using the impact method. Step-like digital bleaching, which occurred at the moment indicated by the arrow, confirms that we actually observed single molecules. The highest resolution we achieved is shown in Fig. 4(c). The diameter of the fluorescence spot was as small as 15 nm, which is less than the aperture diameter evaluated by using a scanning electron microscope as shown in Fig. 4(d). This result is inconsistent with conventional NSOM observations; the optical spot generated at the aperture should be larger than the physical aperture diameter because of the finite penetration of light into the coated metal. One possible explanation for this discrepancy is based on the contribution of energy transfer from an excited molecule to the metal aperture: When the molecule is beneath the metal coating, the energy transfer shortens the fluorescence decay time and thus reduces emission intensity dramatically. On the other hand, no energy is transferred when the molecule is below the aperture hollow. Because the interaction distance in the process of energy transfer is only a few nanometers, we expect to reach a spatial resolution less than 10 nm.

With the recent progress in the nanostructuring of semiconductor materials and in the applications of these nanostructured materials in optoelectronics, NSOM microscopy and spectroscopy have become important tools for determining the local optical properties of these structures. In single-quantum-dot spectroscopy, NSOM provides access to individual quantum dots (QDs), an ensemble of which exhibits inhomogeneous broadening due to the wide intra-ensemble distribution of sizes and strains.[13] NSOM can thus elucidate the nature of QDs, including the narrow optical transition arising from the atom-like discrete density of states. Figure 5(b) is a room-temperature photoluminescence (PL) image of individual self-assembled InGaAs QDs grown on a GaAs substrate, the structure of which is illustrated in Fig. 5(a). A typical PL spectrum of a single QD is shown in Fig. 5(c). At an appropriate excitation density, emission lines from the first excited state (E_{ex}) as well as the ground state (E_g) can be seen. Here we focus on the broadening of homogeneous linewidth, which is determined by the dephasing time of the electron system. Single-QD PL spectra of several tens of QDs were measured and the homogeneous linewidths of ground-state emission are plotted as a function of interlevel spacing energy ($\Delta E=E_{ex}-E_g$) in Fig. 5(d).[14] It can be seen that the homogeneous linewidth increases with ΔE, which reflects the size of QDs (quantum confinement should cause ΔE to increase when the QD size is deceased). Such a dependence of linewidth on QD size can be reproduced by theoretical calculation, and it gives us information important for optimizing the QD size for device applications.

In contrast to the well-defined quantum confined systems such as QDs grown in self-assembled mode, the more common disordered systems with local potential fluctuations still leave open questions. To fully understand such complicated systems from information gained by optical spectroscopic study, we will need a spatial resolution much better than the 100 nm required for conventional NSOM measurement of semiconductor materials. We therefore used an NSOM probe with high collection efficiency for 10-nm imaging spectroscopy of a semiconductor alloy with composition fluctuation. The PL from a single GaNAs quantum well was investigated using NSOM

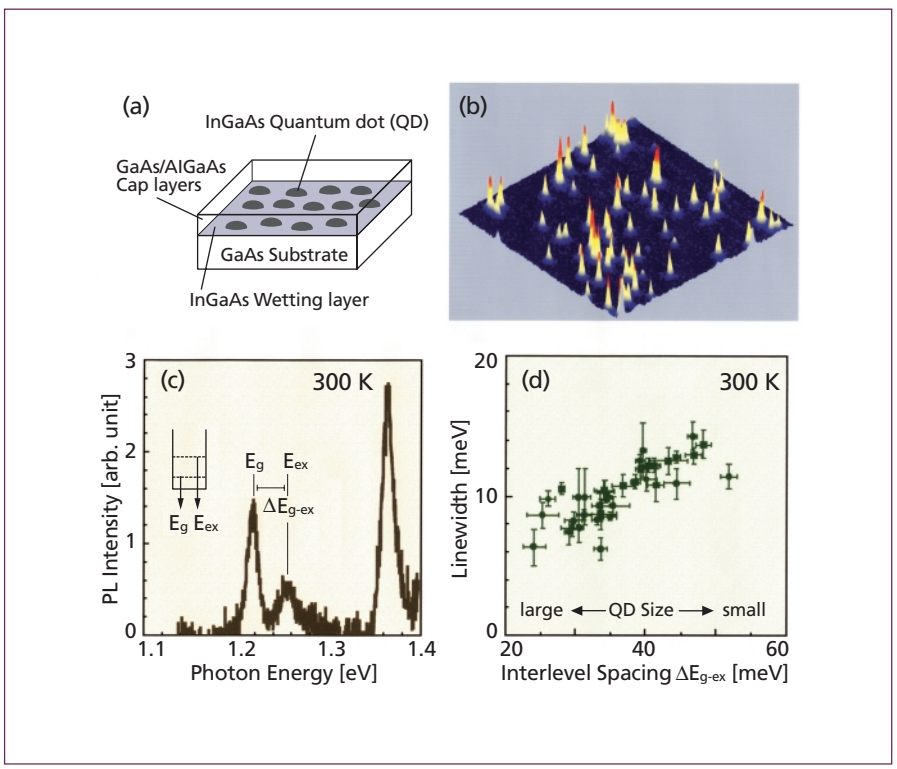

Fig. 5 (a) Sample structure of InGaAs quantum dots (QDs). (b) Room-temperature photoluminescence near-field image of individual QDs. (c) Photoluminescence spectrum of a single QD at room temperature. (d) Dependence of the homogeneous linewidth of ground-state emission on interlevel spacing, which is closely related to the size of QDs.

at cryogenic temperature. Figure 6(a), comparing far-field (macroscopic) and near-field (microscopic) PL spectra measured at 8 K, shows that the broad far-field PL spectrum contains extremely sharp PL lines as well as broad lines. Figures 6(b) and 6(c), monochromatic PL images obtained in two different areas with the PL detection energy fixed at 1.361 eV, show that spatial features of the potential fluctuation are clearly visualized when the resolution is 10 nm. The position dependence of PL spectra in Fig. 6(d) clarifies that such small features correspond to the broader emission while the intensity of narrow emission remains almost constant in the observation area. Localization and delocalization of excitons should be caused by the interface roughness of the quantum well and the compositional variation of nitrogen. Systematic studies will provide insight into the transport and emission properties of complicated electron systems, and it is noteworthy that 10-nm resolution is sufficient for mapping out the exciton wave functions of quantum confined systems.

6. Ultrafast coherent spectroscopy

Time-resolved optical spectroscopy provides a wealth of information on dynamic processes like the phase and energy relaxation of excitons in semiconductor nanostrucures. Real-space diffusion, trapping, and relaxation processes of photogenerated carriers in low-dimensional semiconductors are of interest from the viewpoint of fundamental physics as well as with regard to potential device applications. The combination of femtosecond spectroscopy with NSOM offers new perspectives for the direct investigation of carrier dynamics on the nanometer length scale.

Coherent control of electronic excitation of the quantum confined system is of great importance because of its possible application in quantum information manipulations such as quantum computation. Toda *et al*. performed near-field coherent excitation spectroscopy of a single QD and generated a coherent superposition of carrier wave functions with different energies.[15] They observed an InGaAs self-assembled QD at cryogenic temperature. A PL spectrum of the lowest emission (E_0) and a corresponding PL excitation spectrum with respect to the PL peak are shown in Fig. 7(a). Several sharp lines in the excitation spectrum can be identified as resonant Raman scattering by localized phonons. A femtosecond-pulsed laser was tuned to an energy at which two peaks (peaks E_1 and E_2 in Fig. 7(a)) could be excited simultaneously. As shown in Fig. 7(b), sequence pulses with time delay τ excited the QD through the aperture probe, and the PL signal was collected by the same probe. In Fig. 7(c) the PL intensity de-

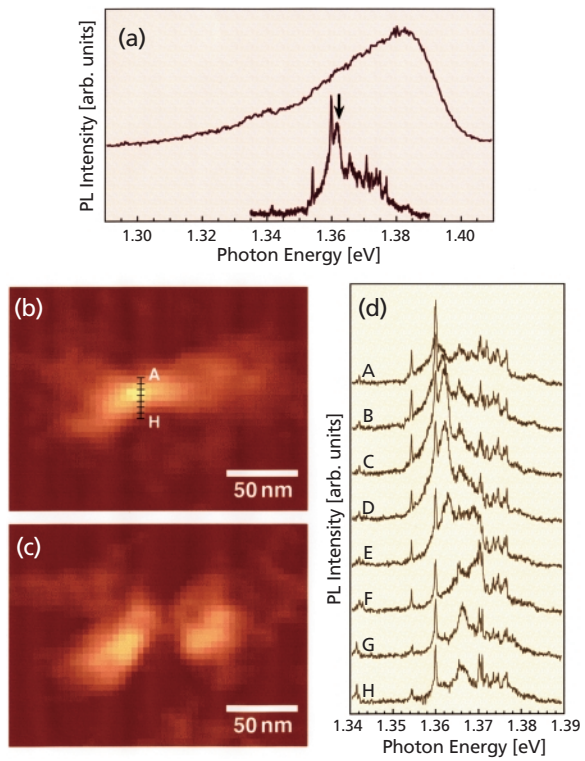

Fig. 6 (a) Photoluminescence (PL) spectra of single GaNAs quantum well with macroscopic far-field detection (upper) and near-field detection (lower). (b) and (c) Near-field PL images obtained in different scanning areas with the detection energy fixed at 1.361 eV (indicated by the arrow in (a)). (d) Position dependence of PL spectra obtained at every 4-nm step from A to H in (b).

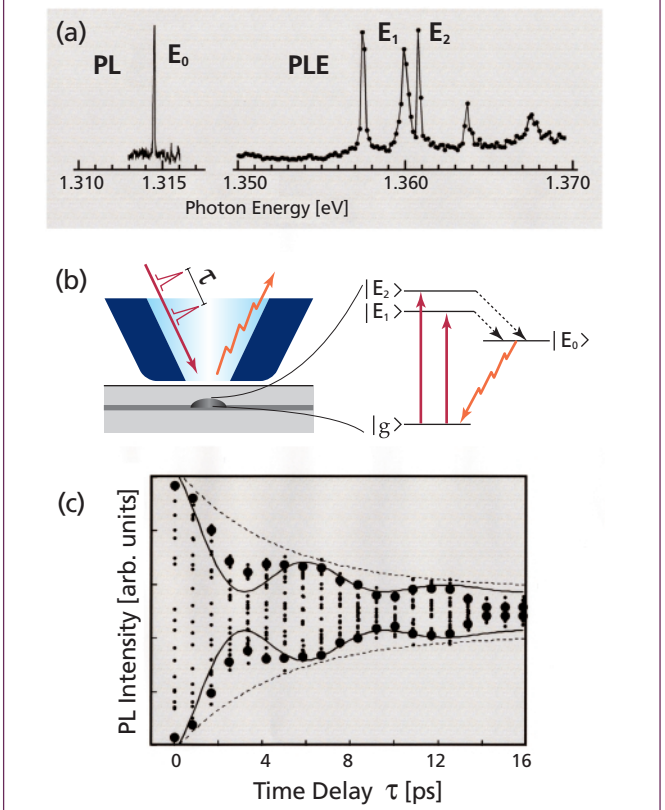

Fig. 7 (a) Near-field photoluminescence (PL) spectrum of a single quantum dot and corresponding PL excitation spectrum. (b) Schematic illustration of two-pulse coherent spectroscopy and an energy diagram of the optical transition involved in this experiment. (c) Quantum beat signal between E_1 and E_2 resonances.

tected is plotted against pulse delay τ. The amplitude of the PL intensities exhibits a slow oscillation superimposed on the exponential decay. The modulation frequency is consistent with the energy separation between the two peaks. Such a beat behavior implies that two closely spaced quantum states are coherently coupled with the ground state has been generated. The estimated decay time (dashed line), which is associated with the lifetime of the localized phonon, is in good agreement with the inverse linewidth of the two resonances.

7. Polarization microscopy

Polarization-contrast NSOM is promising for investigating a variety of material characteristics, such as optical anisotropy, magneto-optical effects and electron spin dynamics. Local polarization control and detection in the nanometer region will be directed toward the development of nano-optoelectronic devices and nano-recording media. One advantage of the tapered fiber probe in polarization NSOM is that the polarization at the aperture, as measured in the far field, can be set to any desired state, with an extremely high extinction ratio. Most conventional polarization spectroscopy can thus be combined with NSOM measurement. Here we describe two novel applications of polarization NSOM: observing the electric field response of liquid crystal (LC) molecules,[16] and imaging phase-change recording marks by using depolarization NSOM.[17]

The physical properties of LC display devices are determined by the interaction between the LC and the alignment layer. To investigate the microscopic nature of this interaction, we developed a type of NSOM suitable for the investigation of local orientation of a LC to which an electric field has been applied. As illustrated in Fig. 8(a), a fiber probe was brought into a droplet of LC and set in close proximity to the alignment layer. The LC orientation at the apex was measured by the change in the polarization state of transmitted light in a crossed Nicols polarization configuration. The metallized tip was also used to apply a uniform electric field to LC molecules in the observation volume.

Figures 8(b) and 8(c) respectively show NSOM images of LC orientation near the damaged alignment layer without and with the applied electric field. The tip-surface distance was maintained at 300 nm by utilizing an optical feedback with evanescent illumination from the backside of the alignment layer. In Fig. 8(b) strong optical contrast is seen in the damaged area. One possible explanation for this contrast is as follows. The dark area, where the alignment layer was pounded by the probe, was seriously damaged and the anchoring effect was reduced there. The intensity of the light transmitted through this area decreased because the LC molecules in the damaged area did not align homogeneously. The alignment layer in the pounded area was squeezed out and into the surrounding region. The bright circular contrast should correspond to this region where the pre-tilt angle is decreased. In Fig. 8(c), on the other hand, there is no contrast due to surface damage because the electric field forces the LC molecules to align vertically.

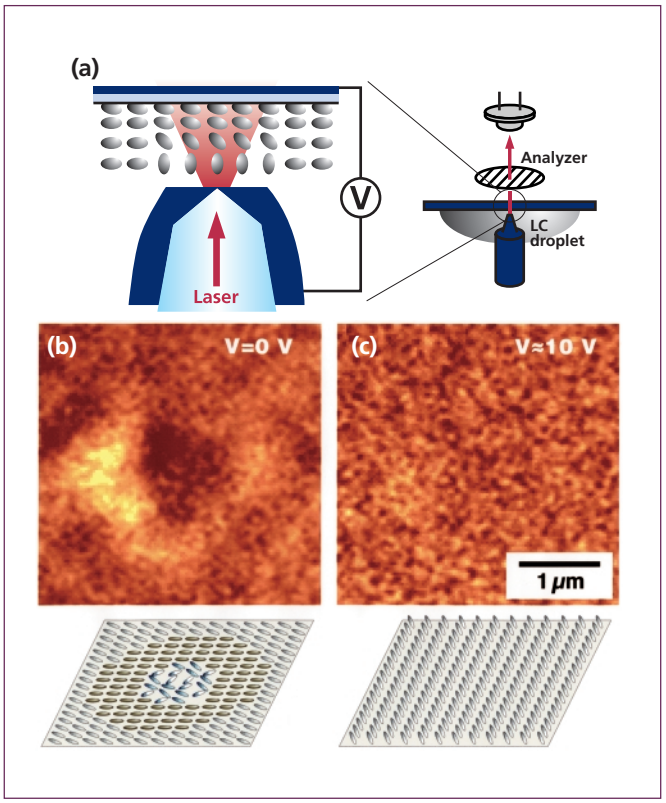

Fig. 8 (a) Experimental configuration for liquid crystal (LC) observation. Near-field imaging of LC orientation on a damaged alignment film (b) without and (c) with an applied voltage.

Reflection-mode NSOM, in which the aperture probe both illuminates the sample and collects the reflected light, is expected to extend the application of NSOM to the industrial field for use in optical data storage and in optical diagnostics (for opaque materials). The difficulty of reflection NSOM is due to its poor optical contrast, which is in turn due to the strong background signal reflected back from the tapered region of the probe. One promising solution is to also use the concept of depolarization NSOM, in which the depolarized (orthogonally polarized) light due to the near-field interaction between the aperture and the sample can be detected as a signal because the background has been suppressed effectively. We used polarization NSOM for high-contrast imaging of DVD-RAM recording marks.

The experimental setup is shown schematically in Fig. 9(a). The polarization of light at the aperture could be controlled by using λ/2 and λ/4 waveplates. The internally reflected background light with ellipsoidal polarization was rejected using a λ/4 waveplate and an analyzer, and the orthogonal component was detected as a signal. Appropriate preparation of the fiber probe enables us to achieve high extinction of background with a ratio in excess of 10^{-5}, as plotted in Fig. 9(b). In this measurement we used an ultrasmall aperture with a diameter of 15 nm, an SEM picture of which is shown as an inset in Fig. 9(a). The sample was a phase-change DVD-RAM medium, where signals are recorded by reversibly changing small regions between the amorphous state and crystal state.

Figures 9(c) and 9(d) are polarization NSOM images of amorphous recording marks written by a blue laser diode. The image in Fig. 9(c) was obtained when the λ/4 waveplate and the analyzer were adjusted to minimize the background signal reflected from the crystal area. Amorphous recording marks are clear, and the contrast between the amorphous area and the crystal area was 8:1, four times the 2:1 contrast obtained in the far-field reflection measurement. To check the polarization state of light reflected from amorphous record-

ing marks, we readjusted the analyzer to minimize the signal in the amorphous area. The extinction ratio reached the same value as that estimated for the crystal area. The image obtained is shown Figure 9(d), where the contrast is as high as in Fig. 9(c). Although the mechanism of contrast generation is not fully understood, such high-contrast imaging of recording marks is intriguing from the viewpoint of recording device applications.

8. Raman spectroscopy

In material science and chemistry, Raman spectroscopy has been widely used to study the distributions of phase and stress as well as to identify molecules and bonds. Raman microscopy is a valuable tool in silicon integrated circuit technology because the Raman shifts are indicative of local stress, which can degrade device performance. As the dimensions of device structures move into the submicron regime, we need Raman spectroscopic measurements with resolution higher than that of conventional techniques. One technical challenge of NSOM Raman spectroscopy is the detection of very low signal levels resulting from the small Raman scattering cross section. This challenge, however, is expected to be met by using a high-transmission probe that delivers several tens of microwatts to a spot on the sample surface 100 nm in diameter and collects the Raman signal with a sensitivity as high as that of an objective with a large numerical aperture.

As a demonstration of the feasibility of NSOM Raman spectroscopy, we show the two-dimensional mapping of the Raman signal of a thin film of polydiacetylene (PDA).[18] The same aperture was used for local illumination of the sample and local collection of the Raman signal. In Fig. 10(a) the near-field Raman spectrum of PDA is compared with the Raman spectrum obtained when the probe was 100 nm from the sample. The result assures us that the aperture probe collects the local Raman signal without any far-field background. Figure 10(b) displays a mapping of Raman intensity at the C=C peak (1460 cm^{-1}). The corresponding topographic image does not exhibit any significant structure or correlation with the Raman image. The properties imaged depend on the polarization geometry, and this dependence is useful when we investigate conformation characteristics such as crystal orientation and the degree of crystallinity of a sample.

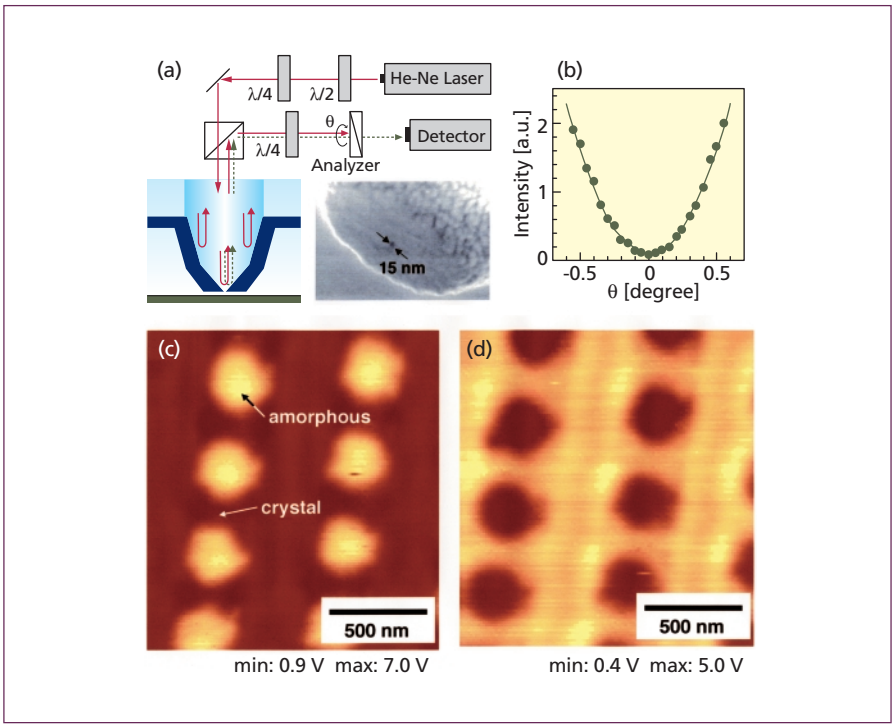

Fig. 9 (a) Schematic diagram of setup for depolarization NSOM in the reflection configuration. The inset is a scanning electron micrograph of the aperture. (b) Evaluation of extinction ratio for rejection of background reflected light. (c) and (d) Near-field images of recording marks of phase-change medium with polarization contrast. The analyzer was adjusted to minimize the background signal either on (c) the crystal area or (d) the amorphous area.

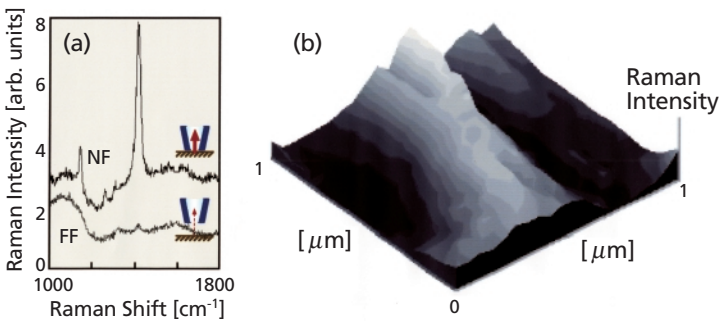

Fig. 10 (a) Raman spectra of polydiacetylene thin film obtained in near-field configuration (upper) and that obtained by positioning the probe 100 nm above the substrate. (b) Near-field mapping of Raman intensity at the C=C peak (1460 cm^{-1}).

Apertureless NSOM with a metallized sharp tip has attracted growing interest among those who want to push the limit of spatial resolution down to 10-30 nm. Since the electric field and the resultant Raman efficiency is drastically enhanced at the tip, better rejection of stray light as well as high resolution can be achieved. Hayazawa *et al*. made Raman images of dye molecules at a 30-nm spatial resolution with a reasonable signal intensity.[19] Their experimental configuration is illustrated in Fig. 11(a). The probe was prepared by metallizing a silicon cantilever with silver, and the apex diameter was approximately 40 nm. Rhodamine 6G molecules cast on a silver island film were used as the sample, and the unwanted background was suppressed by using focused evanescent illumination. Raman peaks of the C-C vibration modes, obtained at steps of 30-nm in the line-scanning, are shown in Fig. 11(b). The appearance of new peaks as well as remarkable changes in peak position and intensity can be seen clearly in some spectra. These features seem to be closely related to both a pure electromagnetic effect and an enhancement due to charge transfer or bond formation.

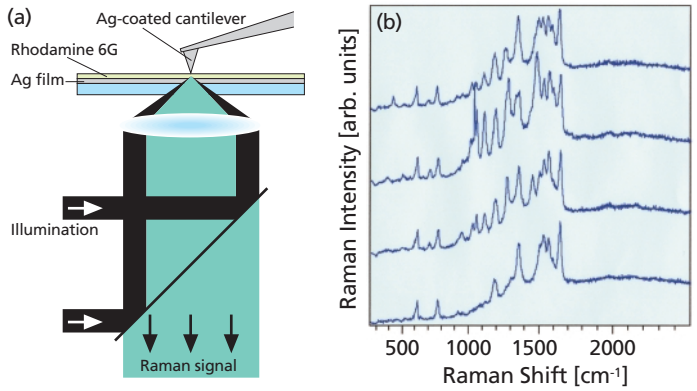

Fig. 11 (a) Schematic drawing of setup for near-field Raman spectroscopy with local field enhancement. (b) Near-field Raman spectra of Rhodamine 6G obtained at every 30-nm step in line scanning.

9. Perspectives

The quality and reproducibility of NSOM measurements have been greatly improved in the last few years by the introduction of high-definition fiber probes made by combining chemical etching with ion-beam milling or by using a simpler impact method. Probes having apertures with diameters as small as 10 nm have been made, and their excellent performance have been demonstrated through high-resolution imaging of semiconductor nanostuructures and single molecules. The probes, however, should be improved with respect to optical transmission, tip stability, and damage threshold. Microfabricated probes offer a promising solution to these difficulties, and are likely to improve experimental reproducibility by providing better defined conditions. Apertureless (or scattering) techniques will surely improve spatial resolution.

The combination of NSOM with a pulsed laser not only makes possible ultrafast time-resolved spectroscopy but also enables us to utilize nonlinear optical processes such as two-photon absorption and second harmonic generation. Such multi-photon techniques can help improve spatial resolution and avoid problems due to stray light. In some cases, NSOM imaging based on the nonlinear optical response gives us information on microscopic structures that is complementary to the information given us by linear optical results. In observation of the domain structure in magnetic thin films, for example, the linear magneto-optics is sensitive to magnetization components perpendicular to the film plane, whereas second-harmonic generation is sensitive to the in-plane magnetization.

Another way to make NSOM more useful is to extend the wavelength region in which it can be used. Ultraviolet light (UV) is very useful in biological studies because certain biomolecules, like DNA and protein molecules, can be observed with direct excitation. UV nano-lithography will also be an important application of NSOM. NSOM infrared spectroscopy with nanometer resolution will be required in a variety of areas in material, molecular, and biological science.

In this article we focused on the spectroscopic applications of NSOM and covered only a small portion of the research currently being pursued in the area of near-field optics. Insight into the nanometer-scale interaction between the mesoscopic electronic system and photons will provide us with the key concepts underlying the operation of nano-optoelectronic devices. For example, the near-field optical coupling of nano-electronic systems can enhance far-field forbidden transitions. Such alternation of selection rule of optical transition will lead to spatiotemporal coherent control of electronic excitation, which can be utilized as the principal function of nanometric devices.[20] Remarkable progress is also being made in industrial applications of NSOM in areas such as optical data storage[21] and optical manufacturing.[22]

Acknowledgements

We are grateful to M. Ohtsu, K. Nishi, H. Saito, M. Takahashi, H. Toriumi, K. Ichihara, K. Yusu, T. Tadokoro, T. Inoue, F. Sato, S. Mononobe, K. Matsuda, N. Hosaka, and K. Ikeda for their assistance and fruitful discussions.

JSAP

References

1) M. Ohtsu, ed.: *Near-Field Nano/Atom Optics and Spectroscopy* (Springer-Verlag 1998).
2) S. Kawata, ed.: *Near-Field Optics and Surface Plasmon Polaritons* (Springer-Verlag 2001).
3) T. Pangaribuan, K. Yamada, S. Jiang, H. Ohsawa and M. Ohtsu: Jap. J. Appl. Phys. **31**, L1302 (1992).
4) S. Mononobe and M. Ohtsu: IEEE Photon. Technol. Lett. **10**, 99 (1998).
5) M. Muranishi, K. Sato, S. Hosaka, A. Kikukawa, T. Shintani and K. Ito: Jpn. J. Appl. Phys. **36**, L942 (1997).
6) T. Saiki and K. Matsuda: Appl. Phys. Lett. **74**, 2773 (1999).
7) T. Saiki, S. Mononobe, M. Ohtsu, N. Saito and J. Kusano: Appl. Phys. Lett. **68**, 2612 (1996).
8) S. Mononobe, T. Saiki, T. Suzuki, S. Koshihara and M. Ohtsu: Opt. Commun. **146**, 45 (1998).
9) T. Yatsui, M. Kourogi and M. Ohtsu: Appl. Phys. Lett. **73**, 2090 (1998).
10) H. Furukawa and S. Kawata: Opt. Commun. **132**, 170 (1996).
11) H. Nakamura, T. Sato, H. Kambe, K. Sawada and T. Saiki: J. Microscopy **202**, 50 (2001).
12) N. Hosaka and T. Saiki: J. Microscopy **202**, 362 (2001).
13) T. Saiki, K. Nishi and M. Ohtsu: Jpn. J. Appl. Phys. **37**, 1639 (1998).
14) K. Matsuda, K. Ikeda, T. Saiki, H. Tsuchiya, H. Saito and K. Nishi: Phys. Rev. B **63**, 121304 (2001).
15) Y. Toda, T. Sugimoto, M. Nishioka and Y. Arakawa: Appl. Phys. Lett. **76**, 3887 (2000).
16) T. Tadokoro, T. Saiki and H. Toriumi: submitted to Jpn. J. Appl. Phys.
17) T. Saiki, K. Yusu, K. Ichihara and T. Tadokoro: submitted to Appl. Phys. Lett.
18) Y. Narita, T. Tadokoro, T. Ikeda, T. Saiki, S. Mononobe and M. Ohtsu: Appl. Spectroscopy **52**, 1141 (1998).
19) N. Hayazawa, Y. Inouye, Z. Sekkart and S. Kawata: Chem. Phys. Lett. **335**, 369 (2001).
20) H. Hori: *Optical and Electronic Process of Nano-Matters*, edited by M. Ohtsu (Kluwer 2001).
21) S. Hosaka, T. Shintani, M. Miyamoto, A. Hirotsune, M. Terao, M. Yoshida, K. Fujita and S. Kammer: Jpn. J. Appl. Phys. **35**, 443 (1996).
22) T. Kawazoe, Y. Yamamoto and M. Ohtsu: Appl. Phys. Lett. **79**, 1184 (2001).